

*J. Mater. Environ. Sci.* 7 (7) (2016) 2572-2582  
ISSN : 2028-2508  
CODEN: JMESC

Shaban et al.



## Electrochemical study of copper corrosion inhibition in acidic environment by 5-(4'-isopropylbenzylidene)-2,4-dioxotetrahydro-1,3-thiazole

A. Shaban<sup>1\*</sup>, Gy. Vastag<sup>2</sup>, A. Pilbáth<sup>1</sup>, I. Kék<sup>1</sup>, L. Nyikos<sup>1</sup>

<sup>1</sup>Functional Interfaces Group, Institute of Materials and Environmental Chemistry, Research Centre for Natural Sciences, MTA, 1117 Budapest, Magyar Tudósok krt. 2., Hungary.

<sup>2</sup>University of Novi Sad, Faculty of Natural Sciences and Mathematics, Serbia.

Received 09 Dec 2015, Revised 15 Jan 2016, Accepted 28 Jan 2016

\*Corresponding author: E-mail: [shaban.abdul@tk.mta.hu](mailto:shaban.abdul@tk.mta.hu) (A. Shaban); Phone: +36 1 3826826

### Abstract

Corrosion inhibition properties of the thiazole derivatives, namely (5-(4'-isopropylbenzylidene)-2,4-dioxotetrahydro-1,3-thiazole) (5-IPBDT), as a corrosion inhibitor for copper in acidic sodium sulphate solution 0.1 M have been studied by electrochemical and electro-gravimetric methods such as potentiodynamic polarization measurements, electrochemical impedance spectroscopy (EIS), electrochemical quartz crystal microbalance (EQCM), and scanning electrochemical microscopy (SECM). The polarization curves showed that the presence of 5-IPBDT successfully reduced the corrosion of copper and this effect increased with increasing the applied concentration. EIS revealed that the presence of inhibitor remarkably increased the impedance of copper electrode over the whole studied frequency range. By obtaining the polarization resistance, the inhibition efficiency of 5-IPBDT as high as 93%, which is in a good agreement with the results obtained by the polarization curves (96%). By using SECM, the formation of the inhibitive film was followed in time. At the open circuit potential, the surface changed gradually from a conductive to an insulating surface in the presence of 5-IPBDT. EQCM studies revealed that the inhibitor shifted the breakdown potential ( $E_b$ ) of copper electrode to more anodic value, reduced the corrosion current density and hindered the electrode mass loss. Both electrochemical and gravimetric data confirmed that the presence of inhibitor decreases the corrosion rate and thus increases corrosion resistance for copper in 0.1 M  $\text{Na}_2\text{SO}_4$  solution.

**Keywords:** thiazoles, SECM, EQCM, EIS, copper corrosion inhibition.

### 1. Introduction

Despite the excellent corrosion resistance of copper, corrosion inhibitors must be applied in order to hinder the damage of metal dissolution in aggressive acidic media [1,2]. The majority of acid inhibitors contain nitrogen (N) sulfur (S) and oxygen (O) atoms among their structure. Organic heterocyclic compounds have had a wide applications in the corrosion inhibition of many metals such as: for copper and its alloys [2-8], iron [9], aluminum [10-11]. The effectiveness of these organic molecules is based on their ability to form a protective film by several mechanisms (i.e. adsorption etc.).

One of the most important groups of five-membered heterocycles including S and N atoms, are Thiazoles. Thiazole can also be considered as a functional group. The Thiazole rings are planar and aromatic and are characterized by a larger pi-electron delocalization and have therefore great aromaticity [12].

The thiazole derivative molecules adsorb probably through the nitrogen or through coordination with surface from the thiazole ring and form the protecting layer. For a metal such as copper, inhibitor molecules containing those atoms, which can form multi-bonds are strongly recommended.

Our previous investigations have shown that the inhibiting efficiency of thiazoles could be improved significantly by substituting with different alkyl groups in the thiazole moiety [13–15]. Namely, the marked increase of inhibiting efficiency was observed for isopropyl-benzylidene-substituted thiazole, as can be seen in Fig. 1. The molecule in interest is 5-(4'-isopropylbenzylidene)-2,4-dioxotetrahydro-1,3-thiazole (5-IPBDT). This effect is due to the electron-donating effect of the phenyl ring, which increases electron density of the thiazole ring. Several other methods were applied in studying copper corrosion inhibition [2]. In this study were performed by using Electrochemical Quartz Crystal Microbalance (EQCM) in order to monitor the adsorption of inhibitor and dissolution of copper over time. EQCM is usually applied in combination with or complementary to other electrochemical techniques for studying protective mechanisms of examined corrosion inhibitors [16–20]. Electrochemical impedance (EIS) measurements were also performed at different immersion times to gain a clearer picture of the processes that were taking place [21].

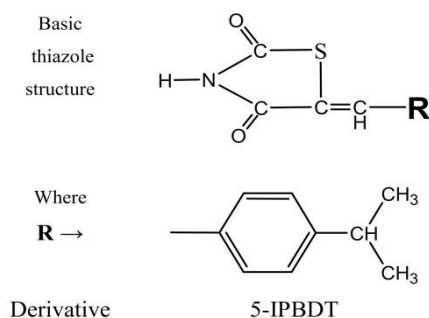


**Figure 1:** The structure of the 5-IPBDT molecule.

Microelectrochemical techniques are becoming essential tools in the study of corrosion reactions, because they provide new in situ information on the processes involved, which are resolved simultaneously in space and time [22–23]. Among the microelectrochemical techniques, the scanning electrochemical microscope (SECM) seems to be most suited for the investigation of such complex systems. It combines the local resolution characteristics of a scanning probe technique with the use of a microelectrode as sensing element, thus providing electrochemical resolution simultaneously. Thus, it is very appropriate to provide in situ electrochemical reactivity information about the surface evolution at the micrometer and sub-micrometer scale in aqueous solution. In addition, SECM has already been used in corrosion science for the detection of anodic and cathodic areas [20], the dissolution of metals [24], and the degradation of organic films [25–28]. Another potential field of application for SECM in corrosion science is to study the formation and destruction of corrosion inhibitor layers [29].

The aim of this work is to report the results from several electrochemical methods that were applied in studying the inhibitive characteristics of 5-(4'-isopropylbenzylidene)-2,4-dioxotetrahydro-1,3-thiazole (5-IPBDT), on copper corrosion in an acidic sulphate containing electrolyte. In order to fulfill this task several electrochemical methods, potentiostatic polarization, EIS, EQCM, and SECM were applied.

## 2. Experimental

### 2.1 Chemicals and solutions

The following materials were used as received: 5-IPBDT, sodium sulphate ( $\text{Na}_2\text{SO}_4$ -Aldrich), (Hydroxymethyl), ferrocene, Ferrocenemethanol (FeMeOH-ABCR GmbH & Co KG). Reagent grade chemicals and Millipore treated water were used to prepare the 0.1 M  $\text{Na}_2\text{SO}_4$  electrolyte. The electrolyte pH was adjusted to 2.95 using diluted sulfuric acid. Due to the low solubility of 5-IPBDT, it was first dissolved into 20 ml of ethanol and then diluted to the desired concentration.

## 2.2 Electrochemical measurements

A three-electrode cell was used for the electrochemical measurements with Cu as the working electrode, SCE as the reference electrode and Pt as the counter electrode. The working electrode was constructed from high purity copper rod (99.99% Cu), with an exposed area of 0.7 cm<sup>2</sup>, embedded in an epoxy resin. The electrode was wet-polished with SiC papers (grit sizes of 800 and 1200), rinsed with acetone and double distilled water, then immersed in the electrolyte solution. Measurements were performed at room temperature according to the procedure described in ASTM G-5-93 standard.

The measurements were carried out when open circuit potential (OCP) was stabilized to 5 mV per 5 minute. The potential was scanned between OCP and 500 mV in both cathodic and anodic directions, at the scan rate of 10 (mVmin<sup>-1</sup>).

The EIS measurements were performed at the OCP with Zahner electric IM5d, after 30 min. of immersion time, in each hour during the 24 hrs period. The applied frequency range was 0.01Hz to 10 KHz, using 10 mV amplitude of sinusoidal voltage. The measurements were performed at an inhibitor concentration 0.01 mM. The impedance spectra were analyzed using program Boukamp EQUIVCRT [30].

## 2.3 SECM measurements

The SECM apparatus was a model of Sensolytics Base (Bochum-Germany). The instrument was operated with a commercial 25 μm gold tip as the probe, an Ag/AgCl / KCl (3 M KCl) reference electrode and a Pt counter electrode. In all SECM measurements potential values are referred to this reference electrode. The substrate material was copper. Wet grinding on silicon carbide abrasive papers (SiC-220 and 4000 grits) was used as surface preparation prior to each measurement. The copper samples were ultrasonically cleaned and rinsed with ethanol. Finally the samples were dried in argon flow. The sample was left at OCP during the measurements.

SECM was applied to study the 5-IPBDT inhibitor layer formation on copper surface. FeMeOH was used as redox-mediator. The measurement of the approach curves were done *in-situ* at OCP in a solution of 0.67 mM FeMeOH and 0.1 M Na<sub>2</sub>SO<sub>4</sub> with the addition of 0.01 mM 5-IPBDT. The study was carried out for 3 hrs, following the layer formation process.

## 2.4 EQCM Measurements

An EQCM system with a 10-MHz AT-cut quartz resonator was used in this study. The EQCM technique allowed us for simultaneous monitoring of volt-amperometric and resonance frequency versus potential characteristics. For thin rigid films, the interfacial mass changes are related to the changes in oscillation frequency of the EQCM through the Sauerbrey equation [31].

The resonator, applied in this our investigation, had gold layers deposited at both sides (thickness 150-nm) over a thin layer of Cr (thickness 15-nm) for adhesive reasons. For each measurement freshly deposited copper layers were galvanostatically electrodeposited on one face of the resonator. The deposition bath contained 0.5 M CuSO<sub>4</sub>, 0.5 M H<sub>2</sub>SO<sub>4</sub>, and 1M C<sub>2</sub>H<sub>5</sub>OH in Millipore ultra-pure water. The cell reference and counter electrodes were SCE and a Pt wire, respectively. The inhibitor concentration was 0.01mM. The cyclic measurements were performed at a potential scan rate of 10 mV/s from E<sub>1</sub> = -500 mV to E<sub>2</sub> = 100 mV, and back to E<sub>1</sub>. The EQCM results were obtained in a simultaneous recording of *i*-*E* and Δ*m*-*E* curves.

## 3. Results and discussion

### 3.1. Polarization results

The percentage of inhibition efficiency (η%) was calculated from the polarization curves based on the following equation:

$$\eta \% = 100 \times (i_{\text{corr},o} - i_{\text{corr},\text{inh}}) / i_{\text{corr},\text{inh}} \quad (1)$$

where *i*<sub>corr,o</sub> is the corrosion current density in the absence of the inhibitor and *i*<sub>corr,inh</sub> is the corrosion current density in the presence of the inhibitor obtained from extrapolating the Tafel plots. Among the investigated concentrations for 5-IPBDT, (1x10<sup>-3</sup>, 3x10<sup>-3</sup>, 5x10<sup>-3</sup>, 7x10<sup>-3</sup> and 1x10<sup>-2</sup> mM), the concentration of 10<sup>-2</sup> mM produced the highest inhibitor efficiency, as can be seen in Fig. 2 and Table 1. The percentage of inhibition

efficiency values increased with inhibitor concentration. The inhibition effect did not change significantly between the concentrations of  $5 \times 10^{-3}$  and  $10^{-2}$  mM, where a plateau started to develop. Due to the low solubility of the chemical in water, the concentration of  $10^{-2}$  mM was applied in the rest of investigations.

**Table1:** Inhibition efficiency of 5\_IPBDT as a function of inhibitor concentration.

Inhibitor Concentration (mM)	$1 \times 10^{-3}$	$3 \times 10^{-3}$	$5 \times 10^{-3}$	$7 \times 10^{-3}$	$1 \times 10^{-2}$
Inhibition Efficiency $\eta$ (%)	67	86	92	94	96

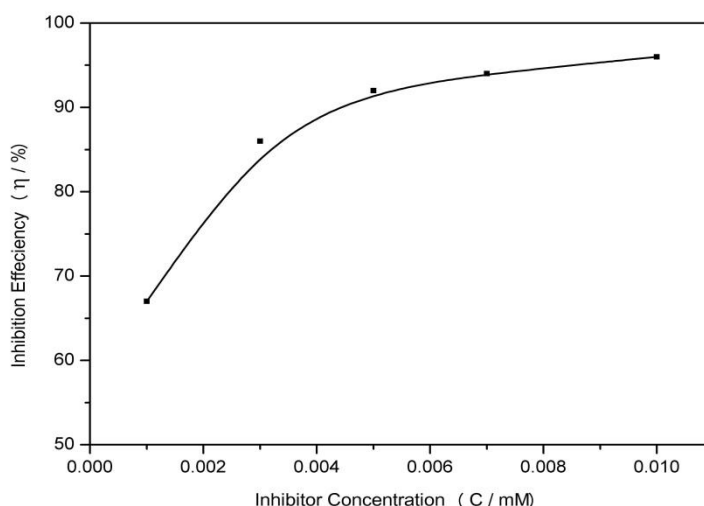


**Figure 2:** Inhibition efficiency of 5-IPBDT against copper corrosion in 0.1 M  $\text{Na}_2\text{SO}_4$  solutions as a function of concentration.

The polarization curves of copper electrode in a 0.1 M  $\text{Na}_2\text{SO}_4$  solution without and with the addition of 5-IPBDT are depicted in Fig. 3. The electrochemical results, obtained from Fig. 3, are summarized in Table 2. The investigated thiazole derivative (5-IPBDT) acted as a cathodic inhibitor against copper corrosion and hindered the oxygen reduction reaction (cathodic reaction) in acidic solution. The addition of 5-IPBDT caused a shift of the electrode corrosion potential ( $E_{\text{cor}}$ ) from  $E_{\text{corr},0} = -52$  mV to  $E_{\text{corr,inh}} = -10$  mV (an anodic shift of 42 mV). Due to the effect of the inhibitor, the value of corrosion current density was reduced from  $I_{\text{corr},0} = 4.9$  to a value of  $I_{\text{corr,inh}} = 0.19 \mu\text{A}/\text{cm}^2$ . This reduction of the current density produced an efficiency of 96% (Table 2).

**Table 2:** Electrochemical results obtained from polarization curves of copper in 0.1 M  $\text{Na}_2\text{SO}_4$  solution without and with the addition of 0.01mM of 5-IPBDT.

Inhibitor	$E_{\text{corr}}$ (mV)	$I_{\text{corr}}$ ( $\mu\text{A}/\text{cm}^2$ )	$B_a$ (mV/deg.)	$B_c$ (mV/deg.)	$\eta$ (%)
0.1 M $\text{Na}_2\text{SO}_4$	-52	4.90	31	191	-
+ 0.01mM 5-IPBDT	-10	0.19	27	204	96

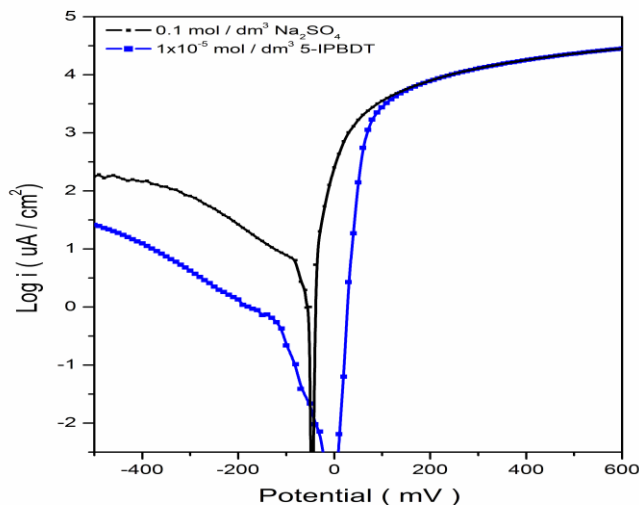


**Figure 3:** Polarization curves for Cu electrode in 0.1 M Na<sub>2</sub>SO<sub>4</sub> without and with the addition of 0.01 mM of 5-IPBDT.

### 3.2 EIS results

EIS is an electrochemical measurement technique which can directly measure the solution resistance ( $R_s$ ), the charge-transfer resistance ( $R_p$ ), and the double-layer capacitance ( $C_{dl}$ ). The Nyquist plots of copper electrode in the electrolyte without and with the addition of the inhibitor shows the depicted polarization resistance value in comparison to the blank solution. The  $R_p$  values were obtained by calculating the semicircle intersection with the real part of the amplitude. The percentage inhibition efficiency ( $\eta\%$ ) was determined using equation 2.

$$\eta (\%) = (1 - R_{p,inh} / R_{p,o}) \cdot 100 \quad (2)$$

where  $R_{p,o}$  and  $R_{p,inh}$  represent the polarization resistance in the absence and presence of the inhibitor in the electrolyte, respectively.

Nyquist plots of copper electrode in 0.1 M Na<sub>2</sub>SO<sub>4</sub> acidic solution in the absence and the presence of 0.01 mM concentration of 5-IPBDT during immersion times of 1 hr and 24 hrs, at room temperature, are shown in Fig. 4-a,b. The depression in the figure is the characteristic of the inhomogeneity of the metal surface during copper corrosion in the acidic sulfate solution [32-34].

Considering the impedance diagrams, polarization resistance ( $R_p$ ) and inhibition efficiency ( $\eta\%$ ) results are given in Table 3. The addition of 5-IPBDT resulted in an  $R_p$  value of 115 k $\Omega$ , comparing that to the blank solution value of 4.9 k $\Omega$ , produced an inhibition efficiency of  $\eta = 93\%$ . This result confirms the previously obtained results.

**Table 3:** Polarization resistance and inhibition efficiency values for copper electrode in 0.1 M Na<sub>2</sub>SO<sub>4</sub> solution in the absence and presence of 0.01 mM of 5-IPBDT.

Solution	Polarization resistance ( $R_p$ ) (k $\Omega$ )	Inhibition efficiency ( $\eta$ ) (%)
0.1 M Na <sub>2</sub> SO <sub>4</sub>	4.9	-
+ 0.01 mM 5-IPBDT	115	93

The change of the polarization resistance values as a function of time is shown in Fig. 5. It is noticed that  $R_p$  values in the presence of the inhibitor increased with time. This is due to the formation of protective layers that hindered the corrosion process. It also shows that time is needed for the inhibitor to adsorb on the copper surface.

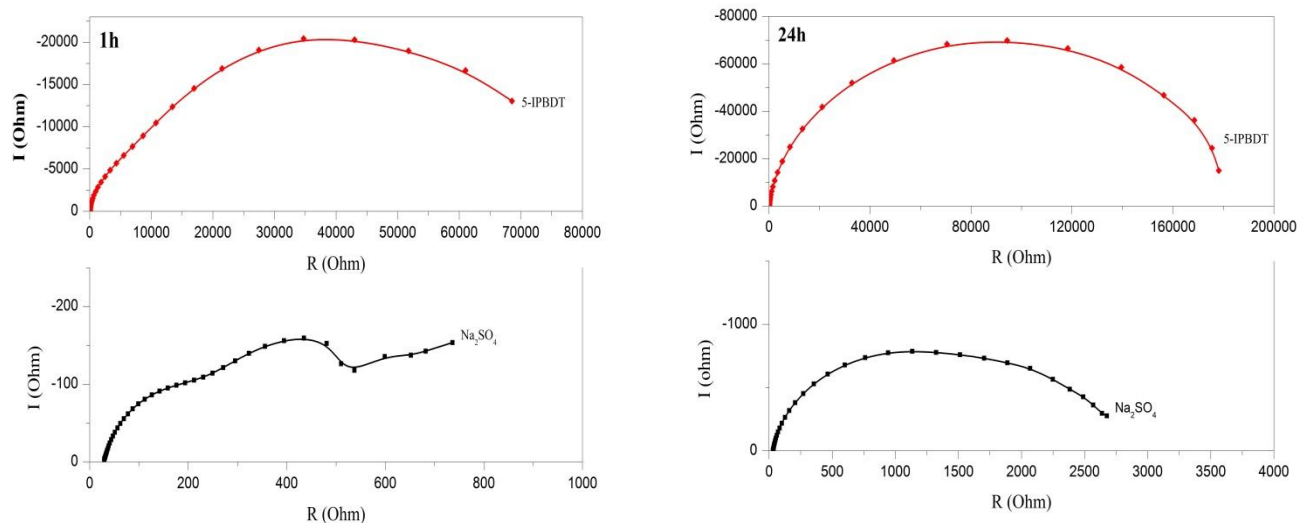


**Figure 4:** Nyquist plots for Cu electrode in 0.1 M Na<sub>2</sub>SO<sub>4</sub> without and with the addition of 0.01 mM thiazole derivatives after 1 hr. (4a) and 24 hrs. (4b) of immersion time.

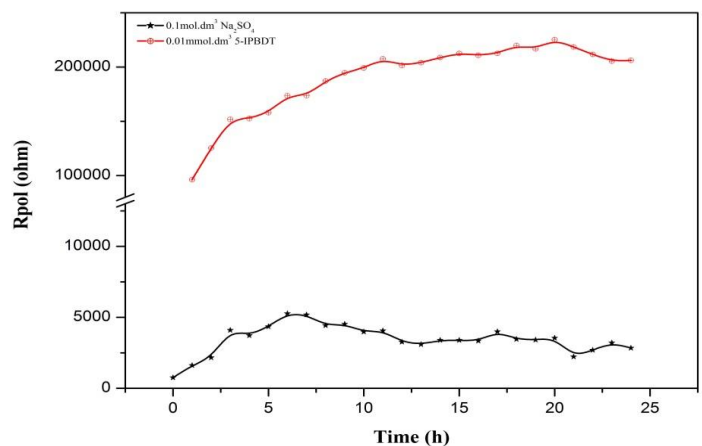


**Figure 5:** The variation of polarization resistance values ( $R_p$ (ohm)) of Cu electrode in 0.1 mM Na<sub>2</sub>SO<sub>4</sub> without and with the addition of 10<sup>-2</sup>mM 5-IPBDT, as a function of immersion time.

The Nyquist impedance plots were analyzed by fitting the experimental data to a simple equivalent circuit model shown in Fig. 6.

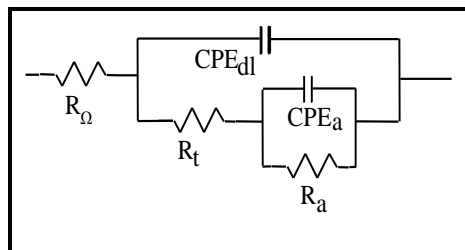


**Figure 6:** Electrical equivalent circuit for the Cu electrode in 0.1 mM Na<sub>2</sub>SO<sub>4</sub> with the addition of 10<sup>-2</sup> mM 5-IPBDT.

In the equivalent circuits,  $R_{\Omega}$  is the solution resistance,  $R_t$  the charge-transfer resistance,  $R_a$  the pseudo-resistance corresponding to the discharge of adsorbed species,  $CPE_{dl}$  represent the double-layer constant phase elements, and  $CPE_a$  the pseudo-constant phase elements. Constant phase elements (CPE) are used to substitute for capacitors to fit the depressed semicircle more exactly.

The Given model describes electrochemical process in both cases, in blank and inhibitor containing solutions, with two relaxation time constants. The first relaxation time constant describes the fast charge transfer process, taking place in the high frequency range [35]. In the high frequency region, the electrode reaction was controlled by a charge transfer process and the diameter of the semicircle represents the charge transfer resistance ( $R_t$ ). The second time constant, in low frequency arc, is a consequence of a charge transfer intermediate adsorption [36]. Results indicated that the corrosion process was controlled mainly by the second time constant in the low-frequency region. The total resistance of the Cu-electrolyte interface ( $R_p$ ), includes  $R_t$  and  $R_a$  values and a real value of the finite diffusion at  $\omega \rightarrow 0$  [37]. The total resistance of the system was used as a measure of the inhibiting efficiency for the inhibitor (5-IPBDT). The values of the elements of the equivalent circuits, obtained by fitting analysis, are tabulated in Table 4.

**Table 4.** Values of the equivalent circuits' elements in Fig.6, after 1 and 24 hrs of immersion time.

Electrolyte	after 1 hr			after 24 hrs		
	$R_p / \Omega$	$C_{dl} / \mu Fcm^{-2}$	$\eta$	$R_p / \Omega$	$C_{dl} / \mu Fcm^{-2}$	$\eta\%$
0.1 M $Na_2SO_4$	749	19.1	0.77	2840	14.3	89
5-IPBDT	74930	5.8	0.93	206200	3.8	96

### 3.3 SECM results

The SECM technique can be employed to study the electrochemical performance of modified electrodes; in this case the bare and 5-IPBDT-modified electrodes are used as the SECM substrate. A mediator such as FeMe-OH is added to the solution, and the tip electrode is operated at a potential where the diffusion-controlled reduction or oxidation, for FeMe-OH, causes a steady-state current at the tip electrode in solution.

In SECM measurements, the recording of the approach curves were done *in-situ* at the free potential in a solution of 0.67 mM FeMeOH and 0.1 M  $Na_2SO_4$  with the addition of 0.01 mM 5-IPBDT, with a commercial 25  $\mu m$  gold electrode.

The base approach curves were performed first in mediator solution (inhibitor and also sodium sulphate free solutions) in order to find the distance where we are close enough to the surface. The next approach curves were done in the inhibitor, sodium sulphate and electrochemical-mediator containing aqueous solutions without changing the tip position in horizontal plane. The formation of inhibitor layer was monitored *in-situ* by the approach curves performed at different immersion times, as seen in Fig. 7.

The activity of the metal has been changed by the formation of the inhibitor layer. Both positive and negative feed-backs (conducting and insulating surface) were obtained during the experiment. The conductive behavior of the uncovered copper changed to an insulating surface, in time, due to the inhibitor layer formation. It can be observed that at early immersion times, until up to 70 min, the amperometric curves showed characteristic positive feedback behavior of free copper present, whereas the SECM tip approaches the surface, which is due to the regeneration of the ferrocene-methanol species on the conductive copper substrate. As the immersion time increased further, the extent of this effect progressively disappears, and the negative feedback behavior becomes characteristic (at higher times than 90 min).

Another form of monitoring the inhibitor film formation in time, from the SECM measurements, is to plot the values of the normalized current measured at the distance of maximum approach as a function of immersion time as shown in Fig. 8. To obtain a better comparison between experiments, the results are shown as a function of normalized tip current. In this procedure the major decrease in current was found to occur during the first 40 min of immersion, and then it decreased further as exposure time increased. The progresses of inhibitor layer

formation in time was proved by the change of the shape of approach curves and by the decrease of the normalized current value measured at a distance of maximum approach, as shown in Fig. 8.

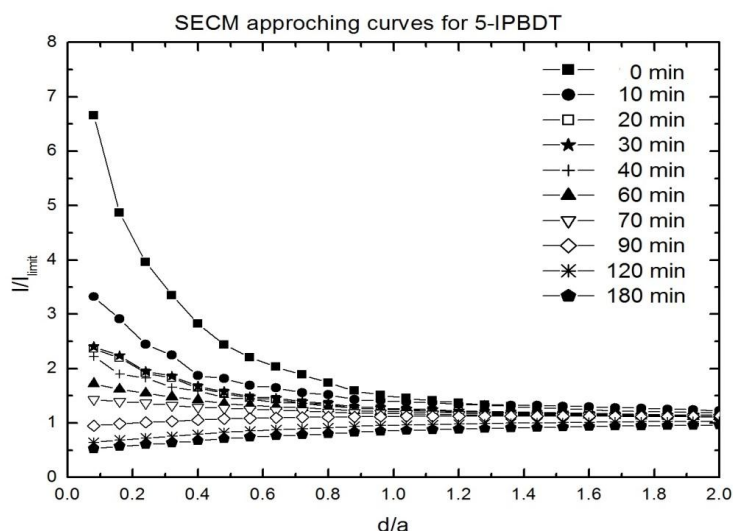


**Figure 7:** Approach curves measured *in-situ* at the Cu substrate in 0.1 M Na<sub>2</sub>SO<sub>4</sub> + 0.67 mM FeMeOH with the addition of 0.01 mM 5-IPBDT, as a function of adsorption time, at a tip potential of +500 mV vs. Ag/AgCl/KCl electrode.

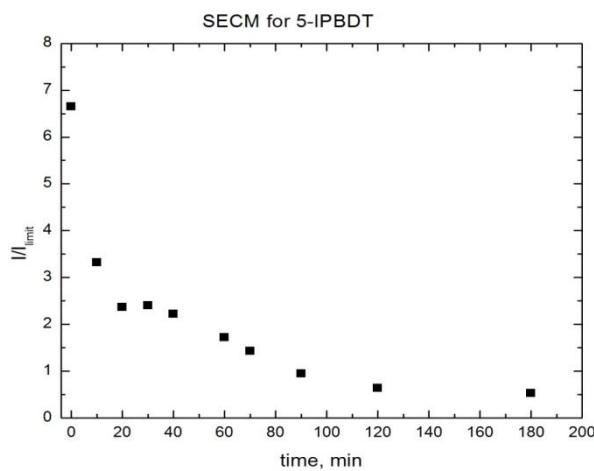


**Figure 8:** Change of the normalized current values measured at the closest distance (0.08 μm) of the tip from the surface, as a function of immersion time.

### 3.4 EQCM results

#### 3.4.1 Effect of 5-IPBDT on Cu corrosion breakdown potential.

The corrosion breakdown potential ( $E_b$ ) is one of the most valuable parameters in providing the means for a quick and reliable comparison of the efficiency of various potential corrosion inhibitors. The breakdown potential is not a static parameter and is normally determined under dynamic conditions, usually using a linear potential scan voltammetry. This technique gives us an indication on the onset of anodic current, however, it is not possible to distinguish between the actual metal dissolution or metal oxide (or salt) scale build-up. Therefore, we applied the EQCM technique and monitored simultaneously the apparent mass variation and current density change as a function of potential which was scanned in the anodic direction. 5-IPBDT containing solution was applied and results (i-E,  $\Delta m$ -E) were registered after the measuring system stabilized, i.e. there is no change in the viscoelastic properties at the interface during measurement.



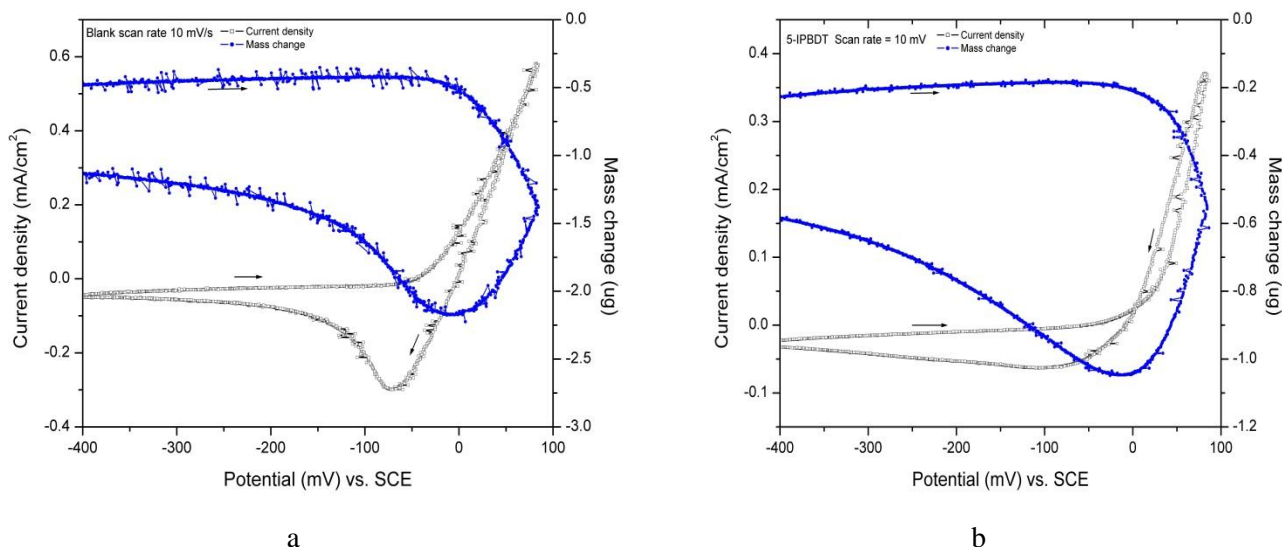


**Figure 9:** Linear potential scan voltammetric and piezogravimetric characteristics of a fresh Cu-EQCM electrode in 0.1 M Na<sub>2</sub>SO<sub>4</sub> without (9a), and with (9b), the addition of 0.01 mM of 5-IPBDT, scan rate = 10 mV s<sup>-1</sup>.

Figure 9 shows voltammetric and piezogravimetric characteristics of freshly deposited Cu-EQCM electrode surface in 0.1 M Na<sub>2</sub>SO<sub>4</sub> without and with the addition of 0.01 mmol.dm<sup>-3</sup> of 5-IPBDT recorded at a scan rate = 10 mV.s<sup>-1</sup>. Electrochemical and gravimetric results obtained from Fig. 9, are tabulated in Table 5.

As shown in Table 5, the addition of 5-IPBDT shifted the break potential from  $E_{b,o} = -47$  mV for the blank solution to a value of  $E_{b,inh} = +5$  mV in the presence of the inhibitor. This resulted in a shift of  $\Delta E_b = 52$  mV to more anodic direction. The electrode mass loss was smaller in the case of the presence of 5-IPBDT ( $\Delta m_{inh} = 0.8$  µg) than that in the blank solution ( $\Delta m_o = 1.85$  µg). The mass loss decrease signifying that the predominant process above the breakdown potential is the copper dissolution from the electrode surface. The copper dissolution continues up to the anodic reversal potential of +100 mV. On backwards cathodic scan, further mass decrease is observed. A small reduction peak can be seen on the  $i$ - $E$  curve but the corresponding mass change is less than the current density demanded (Fig. 9 a).

**Table 5.** Characteristics of Cu-EQCM electrode in 0.1 M Na<sub>2</sub>SO<sub>4</sub> solution without and with the addition of 5-IPBDT.

Solution	$E_B$ (mV)	$\Delta m$ (µg)	( $\eta$ %)	$i_{max}$ (mA/cm <sup>2</sup> )	( $\eta$ %)
0.1 M Na <sub>2</sub> SO <sub>4</sub>	- 47	-1.8	-	0.50	-
+ 0.01mM 5-IPBDT	+ 5	-0.8	56	0.35	57

Figure 9 b also showed that there was no reduction peaks in the reverse cathodic scan direction which is another indication that 5-IPBDT was strongly adsorbed to the copper electrode surface.

It can be also seen in Figure 9, that the electrode mass does not return to the initial value in all cases. This can be attributed to either that the starting scan potential should be more negative and/or that a thin layer, or even a partial layer, of the inhibitors was adsorbed on the surface forming Cu-5-IPBDT layer that hinders the redeposition of the dissolved copper ions.

The high inhibitory efficiency of 5-IPBDT derivative can be related to the presence of the isopropyl group in the molecule, which has a consequence of positive inductive and resonance effects, accompanied by hyperconjugation. In organic chemistry, hyperconjugation is the interaction of the electrons in a sigma bond (usually C-H or C-C) with an adjacent empty (or partially filled) non-bonding p-orbital or antibonding  $\pi$  orbital or filled  $\pi$  orbital, to

give an extended molecular orbital that increases the stability of the system. Only electrons in bonds that are  $\beta$  to the positively charged carbon can stabilize a carbocation by hyperconjugation [38, 39].

## Conclusions

The inhibition of copper corrosion in 0.1 M Na<sub>2</sub>SO<sub>4</sub> using 0.01 mmol.dm<sup>-3</sup> of (5-(4'-isopropylbenzylidene)-2,4-dioxotetrahydro-1,3-thiazole) was studied by several electrochemical methods.

EQCM results, in the form of linear potential scan voltammetric and piezogravimetric characteristics of fresh 5-IPBDT films, showed the degree of protection of 5-IPBDT and the high efficiency against copper corrosion.

SECM results showed that this method can be employed for the characterization of thin 5-IPBDT inhibitor films formed on the copper electrode surface in time. The results of Z-approach curves at different exposing times showed the process of film formation and the change of the conductive characteristics to an insulating characteristic over time.

All applied electrochemical methods showed similar behavior of the copper electrode in the electrolyte solution in the presence of 5-IPBDT, high inhibition efficiency, formation of a thin protective layer, and altering the electrochemical properties of the surface.

The results showed that the inhibition occurred via chemisorption of the inhibitor molecules on the corroding metal and the adsorption process involved the electron donation from the inhibitor to the metal surface.

**Acknowledgments**-The authors are pleased to acknowledge the MTA, TTK, AKI, for providing financial support throughout the research work.

## References

1. Zhang D.-Q., Gao L.-X., Zhou G.-D., *J. Appl. Electrochem.*, 33 (2003) 361-369.
2. Antonijevic M., Petrovic M., *Int. J. Electrochem. Sci.* 3 (2008) 1-28.
3. Finšgar M., Milošev I., *Corros. Sci.*, 52, (2010), 2737-2749.
4. Otmacic H., Stupnisek-Lisac E., *Electrochim. Acta*, 48, (2003) 985-991.
5. Varvara S., Muresan L., Rahmouni K., Takenouti H., *Corr. Sci.*, 50, (2008) 2596-2604.
6. Rahmouni K., Hajjaji N., Keddami M., Srhiri A., Takenouti H., *Electrochim. Acta*, 52, (2007) 7519-7528.
7. Sherif E. M., Erasmus R. M., Comins J. D., *J. Coll.Int. Sci.*, 311, (2007)144-151.
8. Dermaj A., Hajjaji N., Joiret S., Rahmouni K., Srhiri A., Takenouti H., Vivier V., *Electrochim. Acta*, 52, (2007) 4654-4662.
9. Khadraoui A., Khelifa A., Touafri L., Hamitouche H., Mehdaoui R., *J. Mater. Environ. Sci.* 4 (2013) 663.
10. Hari Kumar and S. Karthikeyan., *J. Mater. Environ. Sci.* 3 (5) (2012) 925-934.
11. Hadi Z.M. Al-Sawaad, Alaa S.K. Al-Mubarak, Athir M. HaddadI., *J. Mater. Environ. Sci.* 1 (4) (2010) 227-238.
12. Metzger J. V., Ed., *Chemistry of Heterocyclic Compounds: Thiazole and Its Derivatives*, Part 1, 34, John Wiley and Sons Ltd, UK (2007).
13. Vastag Gy., Szöcs E., A. Shaban, E. Kálmán, *Pure Appl. Chem.*, 73 (2001) 1861-1869.
14. Vastag Gy., Szöcs E., Shaban A., Bertóti I., Popov-Pergal K., Kálmán E., *Solid State Ionics*, 141-142 (2001) 87-91.
15. Telegdi J., Shaban A., Kálmán E., *Electrochim. Acta*, 45, No. 22-23 (2000) 3639-3647.
16. Scendo M., *Corros. Sci.* 49 (2007) 2985.
17. Scendo M., *Corros. Sci.* 50 (2008) 2070.
18. Shaban A., Kalman E., Telegdi J., *Electrochim. Acta* 43 (1998) 159-163.
19. Qafsaoui W., Blanc C., Pebere N., Takenouti H., Srhiri A., Mankowski G., *Electrochim. Acta*, 47 (2002) 4339.
20. Rahmouni K., Keddami M., Srhiri A., Takenouti H., *Corros. Sci.* 47 (2005) 3249.
21. Joseph Raj X., Rajendran N., *J. Mater. Environ. Sci.* 5 (1) (2014) 215-224
22. Marcus P., Mansfeld F., (Eds.), *Analytical Methods in Corrosion Science and Engineering*, CRC Press, Boca Raton, FL, 2006.

23. Oltra R. in: Oltra R., Maurice V., R. Akid and P. Marcus (Eds.), *Local probe techniques for corrosion research*, E. F. C. Publications, 45, CRC Press, Woodhead Publishing and Maney Publishing, Cambridge, England, (2007).
24. Simões A. M., Bastos A. C., Ferreira M.G., González-García Y., González S., Souto R. M., *Corros. Sci.* 49 (2007) 726.
25. Fushimi K., Seo M., *Electrochim. Acta*, 47 (2001) 121.
26. Souto R. M., González-García Y., González S., Burstein G.T., *Corros. Sci.* 46 (2004) 2621.
27. Bastos A.C., Simões A.M., González S., González-García Y., Souto R.M., *Prog. Org. Coat.* 53 (2005) 177.
28. Souto R., González-García Y., González S., *Corros. Sci.* 47 (2005) 3312.
29. Souto R., González-García Y., González S., Burstein G.T., *Electroanalysis* 21 (2009) 2569.
30. Souto R., González-García Y., Izquierdo J., González S., *Corros. Sci.* 52 (2010) 748.
31. Boukamp, B.A.; Equivalent Circuit - EQUIVCRT Program-User's Manual (University of Twente-Holland) v3. 97, 1989.
32. Sauerbrey G., *Z. Phys.* 155 (1959) 206.
33. Feng Y., Siow K.S., Teo W.K., Hsieh A.K., *Corros. Sci.* 53 (1997) 389.
34. Wang D.K.Y., Coller B.A., MacFarlane D.R., *Electrochim. Acta* 38 (1993) 2121.
35. Barcia O., Mattos O., Pebere N., Tribollet B., *J. Electrochem. Soc.* 140 (1993) 2825.
36. Feng Y., Teo W., Siong K., Tan K., Hsieh A., *Corros. Sci.* 38 (1996) 369.
37. Metikoš-Huković M., Babić R., Paić I., *J. Appl. Electrochem.* 30 (2000) 617.
38. Carey F. A., *Organic Chemistry*, McGraw-Hill Companies, 7<sup>th</sup> ed., (2007).
39. Vastag Gy., Shaban A., Felhősi I., Kálmán E.; *ZASTITA MATERIJALA*, 53 (broj 1) (2012) 29-32.

(2016); <http://www.jmaterenvironsci.com/>